Inorganic Chemistry

Article

pubs.acs.org/IC

Co^{2+}/Co^{+} Redox Tuning in Methyltransferases Induced by a Conformational Change at the Axial Ligand

Manoj Kumar,[†] Neeraj Kumar,[†] Hajime Hirao,[‡] and Pawel M. Kozlowski*,[†]

[†]Department of Chemistry, University of Louisville, Louisville, Kentucky 40292, United States

[‡]Division of Chemistry and Biological Chemistry, School of Physical and Mathematical Sciences, Nanyang Technological University, 21 Nanyang Link, Singapore 637371

Supporting Information

ABSTRACT: Density functional theory and quantum mechanics/molecular mechanics computations predict cob(I)alamin (Co^{+}Cbx), a universal B_{12} intermediate state, to be a pentacoordinated square pyramidal complex, which is different from the most widely accepted viewpoint of its tetracoordinated square planar geometry. The square pyramidality of Co^{+}Cbx is inspired by the fact that a Co^{+} ion, which has a dominant d^8 electronic configuration, forms a distinctive Co^{+}--H interaction because of the availability of appropriately oriented filled d orbitals. This uniquely H-bonded Co^{+}Cbx may have catalytic relevance in the context of thermodynamically uphill Co^{2+}/Co^{+} reduction that constitutes an essential component in a large variety of methyltransferases.

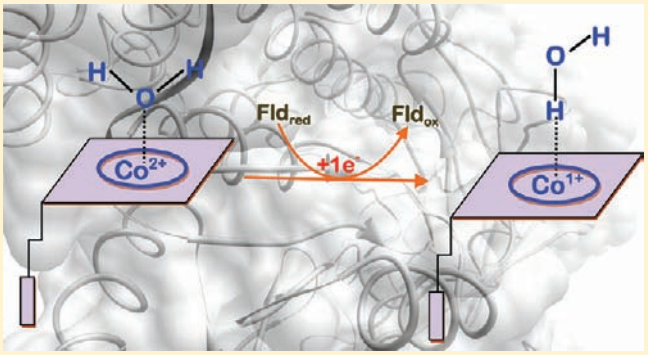

INTRODUCTION

The Co^{2+}/Co^{+} reduction not only lies at the core of the corrinoid chemistry executed by cytoplasmic methyltransferases such as methionine synthase (MetH),[1] methanol-dependent cobalamin,[2] corrinoid/Fe−S protein[3] and others[4] but also forms an essential component of the mitochondrial adenosylation reactions conducted by ATP:corrinoid adenosyltransferases (ACAs)[5] such as human-type CobA,[6] PduO,[7] and EutT.[8] Despite its broad and general chemical appeal, the Co^{2+}/Co^{+} reduction remains poorly understood. This is because Co^{2+}/Co^{+} conversion is a thermodynamically challenging process due in part to the reduction potential of the unbound base-off cob(II)alamin (Co^{2+}Cbx)[9] (−500 mV vs a standard hydrogen electrode (SHE) in water solution) being inaccessible by the physiological reducing agents (−260 to −460 mV vs SHE) operative under cellular conditions.[10−12]

On the basis of structural[13] and spectroscopic evidence,[14−16] formation of tetracoordinated square planar Co^{+}Cbx[9] has been advocated as the most plausible mechanistic description to rationalize the enzyme-mediated tuning of the reduction process in the case of methyltransferases (Scheme 1a). Though such a mechanistic description significantly advances our understanding of Co^{2+}/Co^{+} conversion, there are studies[17−19] indicating that Co^{+}Cbx may also exist in other coordination geometries. Notably, two pentacoordinated Co^{+}-model compounds (i.e., $[pyCo^{+}(dmgBF_2)_2]^-$ and $[MeCNCo^{+1}(dmgBF_2)_2]^-$)[17,18] and a hexacoordinated Co^{+} clathrochelate ($[Co^{+}(Cl_2g)_3(Bn\text{-}C_4H_9)_2]^-$)[19] in a trigonal prism arrangement have been structurally characterized. Further, a growing body of experimental and theoretical evidence[20−23] suggests that d^8 metal ions, such as Pt^{2+} and Co^{+}, can display square pyramidality because of their distinct H-bond forming ability.

Scheme 1. Possible Mechanistic Routes for the Enzyme-Bound Co^{2+}/Co^{+} Reduction in Methyltransferases

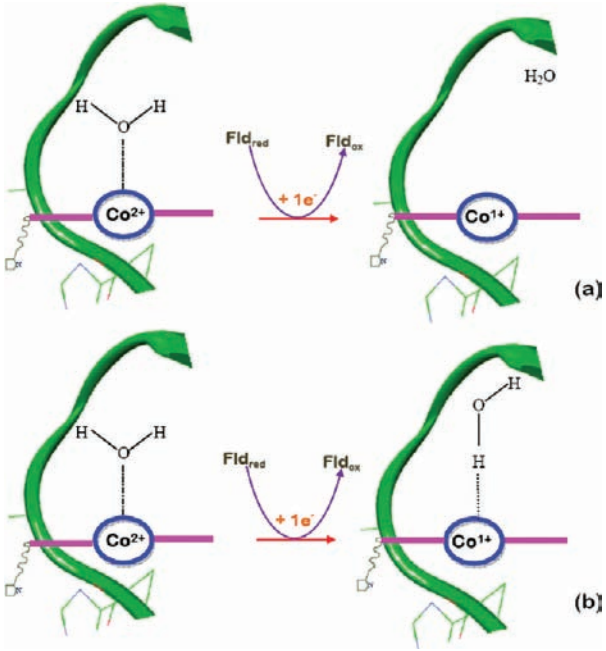

Received: September 7, 2011
Published: May 1, 2012

   dx.doi.org/10.1021/ic201970k | *Inorg. Chem.* 2012, 51, 5533−5538

Importantly, Kozelka et al.[21] have provided the first conclusive evidence of a dispersion driven O−H--Pt^{2+} interaction in an uncharged *trans*-$[PtCl_2(NH_3)(N\text{-glycine})]\cdot H_2O$ complex.

Taking into account these findings, an alternate mechanism for Co^{2+}/Co^{+} redox process has been recently proposed wherein the H-bonded square pyramidal Co^{+}Cbx--H_2O intermediate has been invoked to tune the reduction process.[22] Scheme 1b shows the proposed mechanistic route that involves a conformational change at the axial H_2O ligand rather than its complete dissociation from the cofactor during the course of reaction. The formation of the Co^{+}Cbx--H_2O complex is facilitated by the fact that the Co^{+} ion, which is a dominant d^8 system,[24,25] prefers to deploy its filled d orbitals for constructing a distinctive Co^{+}--H interaction that has noticeable charge transfer, dispersion, and electrostatic components. The density functional theory (DFT) calculations[22] indicate that the Co^{+}--H interaction exerts a sizeable amount of redox tuning (50−225 mV vs SHE) upon the Co^{2+}/Co^{+} process, thereby making it accessible by the common biological reductants.

This short computational paper demonstrates how the plausible mechanistic path shown in Scheme 1b may be realized inside the enzymes, i.e., precisely how the conformational change at the axial ligand may be induced en route to the formation of enzyme-bound Co^{+}Cbx. Herein, we employ DFT, atoms in molecule (AIM), and ONIOM-based quantum mechanics/molecular mechanics (QM/MM) methods to investigate the molecular details of a Co^{+}--H bond formation during the reactivation cycle of the MetH enzyme, which is one of the better understood methyltransferases.[4]

COMPUTATIONAL DETAILS

Model DFT Calculations. All calculations were performed using HF and a variety of DFT functionals (BP86,[26] B97-1,[27] B98,[28] B97-D,[29] ωB97X,[30] and ωB97X-D[31]) and the 6-31++G(d,p) basis set as embroidered into the Gaussian 09[32] quantum chemical suite of programs for electronic structure and properties calculations, except for the AIM analysis that was carried out using AIM2000[33] software. The use of the long-range and the empirical dispersion-corrected DFT functionals (ωB97X, ωB97X-D, and B97-D) was motivated by the fact that the noncovalent interactions had not been faithfully reproduced using conventional DFT.[34] Considering that the crystal structure of Co^{+}Cbx had yet not been resolved, the employed simplified structural models of Co^{+}Cbx (Co^{+}Cbl) as well as those of Co^{2+}Cbx (Co^{2+}Cbl) were prepared from the high-resolution X-ray crystal structure of isolated Co^{2+}Cbx[35] and were further improved by performing the geometry optimization. These structural models were constructed by removing all of the amide side chains and the nucleotide loop of the cofactor. To mimic the possible active site interactions of the upper axial ligand (H_2O), two types of the structural models were considered: (1) Co^{+}Cbl−H_2O−H_2O and Co^{2+}Cbl−H_2O−H_2O, where a H_2O molecule, a universal H-bond donor, was placed in the vicinity of the axial ligand to replicate its H-bonding interaction with the proximal residues, and (2) Co^{+}Cbl−H_2O−HOPh and Co^{2+}Cbl−H_2O−HOPh, where PhOH was used to model the local Y1139 residue of the MetH enzyme. The latter kind of structural models presented an excellent case study platform for extracting valuable insight into the catalytic role of Y1139 residue in relation to the MetH-catalyzed reduction process.[13,15] All of the structural models were fully optimized using the 6-31++G(d,p) basis set, and their optimized geometries were validated to be global minima via frequency calculations. It should be noted that the optimization of Co^{2+}Cbl and Co^{+}Cbl complexes was initiated using O-ended as well as H-ended geometries of H_2O or PhOH interacting with the axial H_2O ligand. Both the starting points converged to the same final structure; i.e., in Co^{2+}Cbl complexes, the neighboring H_2O or PhOH interacted with the axial ligand via its O end, while in Co^{+}Cbl complexes, the local motif communicated through its H end. To analyze the stability of Co^{+}Cbl complexes, the static thermodynamic data were computed supposing a standard state convention of 1 atm and a temperature of 298.15 K. The solvation of Co^{+}Cbl complexes was studied using chloroform (ε = 4.70) solvent within the polarizable continuum model formalism of Gaussian 09.

ONIOM (QM/MM) Calculations. A recently resolved X-ray crystal structure of MetH-bound Co^{2+}Cbx (PDB code: 3IVA @2.7 Å resolution)[13] was used to build a computational model. The experimental artifacts were deleted from the X-ray crystal structure, and consequently, no counterions were included in the models investigated. The H-atoms were subsequently added to the prepared protein model considering the normal protonation state of all titrable residues except histidine. The protonation states of histidine residues were determined at pH = 7.0 using the PROPKA suite of program[36] and visual inspection as follows: HID759, HID841, HID1028, HIE1104, HIE1145, HIE1184, HIP894, HIP927, HIP1021, HIP1027, HIP1080, and HIP1160. HID and HIE were used here to mean that these were neutral histidine residues with the protonated $N_{\delta 1}$ and $N_{\delta 2}$ atoms, respectively, and HIP was a doubly protonated histidine. However, aspartic acid and glutamic acid residues were assumed as ionized, and lysine and arginine residues were assumed as protonated. The crystal H_2O molecules were also included in the model. The model structure was first pre-equilibrated and was subsequently subjected to geometry optimization of the hydrogen atoms using the AMBER force field as implemented in Gaussian 09. Subsequently, AMBER geometry optimization was performed for hydrogen atoms and heavy atoms of the side chains. Merz−Kollman electrostatic potential atomic charges were determined for the cofactor,[37] applying the ONIOM(B3LYP/6-31G(d):AMBER) mechanical embedding (ME) scheme. In this calculation, the cofactor was defined as the model system to which DFT was applied, and the radius for the Co ion was set at 0.79 Å. The residues within 20 Å of the Co center and hydrogen atoms were then geometry optimized with the ONIOM-ME method, where the cofactor was assumed the model system. The Co^{2+}Cbx model turned out to be neutral. Then, the model system was changed as shown in Figure 1, and only the QM atoms were optimized using ONIOM-ME.

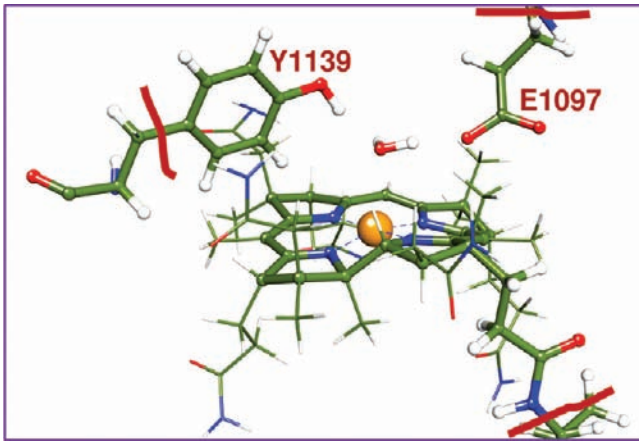

Figure 1. QM:MM partition scheme used in the present ONIOM analysis. The red curly lines represent the boundaries between the QM and MM domains. Here, the QM region is described by DFT, while the MM part is analyzed using the AMBER force field.

After these preparatory calculations, ONIOM electronic embedding (EE) calculations were carried out where the QM part was analyzed using four different functionals (B3LYP, BP86, ωB97X, and ωB97X-D) and 6-31G(d) basis set.

RESULTS AND DISCUSSION

DFT and QM/MM Analysis of Co^{2+}Cbx Models. The optimized isolated Co^{2+}Cbl complexes (Co^{2+}Cbl−OH_2−OH_2 and Co^{2+}Cbl−OH_2−HOPh) were found to be O-bound at the

dx.doi.org/10.1021/ic201970k | Inorg. Chem. 2012, 51, 5533−5538

β face of the corrin ring with a strong Co^{2+}–O (~2.25–2.55 Å) bond (Figure 2; Tables S1 and S2, Supporting Information),

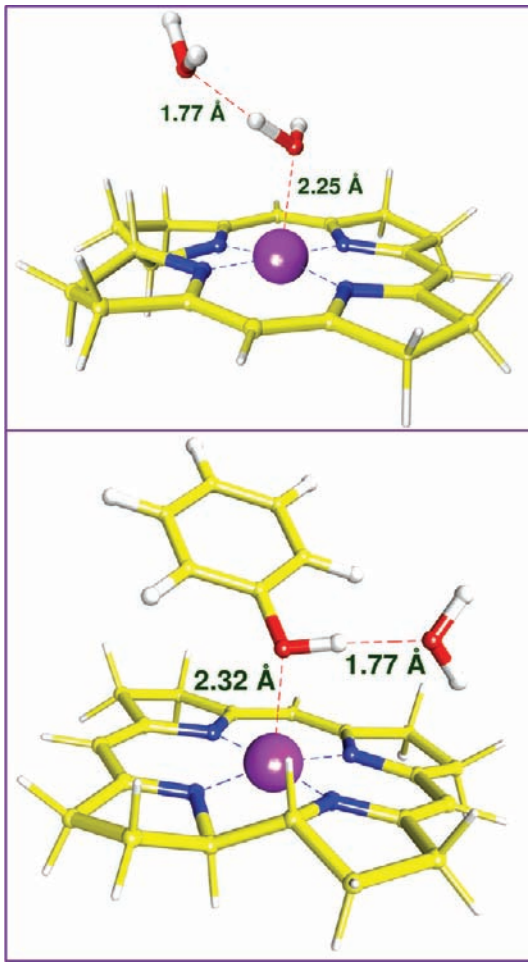

Figure 2. BP86-optimized Co^{2+}Cbl structural models (Co^{2+}Cbl–OH_2–OH_2 (upper); Co^{2+}Cbl–OH_2–HOPh (lower)).

implying that MetH-bound Co^{2+}Cbx would prefer to be O-bound with the axial ligand endorsing prior structural,[13] spectroscopic, and computational studies.[14−16] Note here that the axial H_2O ligand in the optimized Co^{2+}Cbl–OH_2–HOPh complex was displaced by the PhOH moiety that formed a relatively weak Co^{2+}–O bond (~2.32–2.46 Å).

With the ONIOM-based QM/MM calculations, a similar conceptual picture was obtained; i.e., the axial H_2O ligand communicated with the Co^{2+} ion through its O end (Figure 3). The QM/MM optimized Co^{2+}–O bond, ranging between 2.44 Å and 2.66 Å, was noticeably lengthened in comparison to that in the isolated structural models (~2.25–2.55 Å), implying that the enzyme environment would tend to weaken the interaction between the cofactor and the axial ligand. This computational finding is also supported by the existing spectroscopic data of Brunold et al.,[15] where it has been shown that the enzyme environment causes the elongation of Co^{2+}--O bond by 0.2 or 0.3 Å and results in the formation of a weakly bound pentacoordinated Co^{2+}Cbx–OH_2. It should be noted that the QM/MM optimized Co^{2+}–O bond distance was significantly deviated from the experimental value reported in ref. 13 (Figures 3 and S1).[38] This discrepancy between the calculated and the experimental data might be

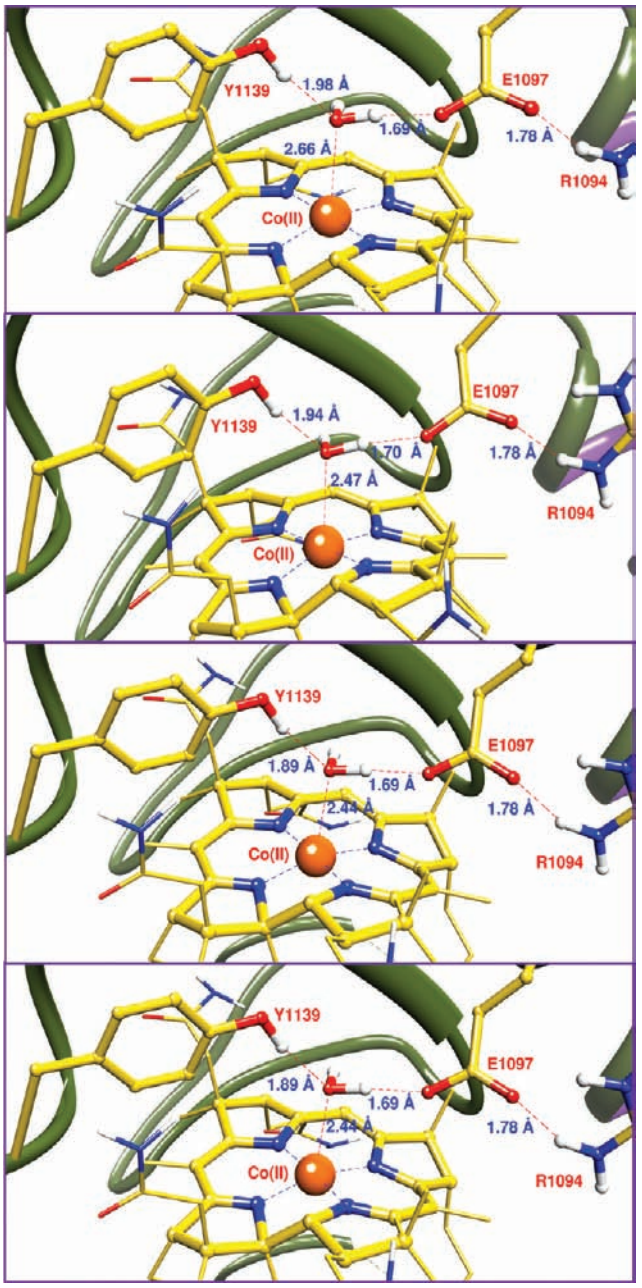

Figure 3. Active site view of the ONIOM (DFT:AMBER) optimized MetH-bound Co^{2+}Cbx (DFT = B3LYP/6-31G(d) (top), BP86/6-31G(d) (middle 1), ωB97X/6-31G(d) (middle 2), and ωB97X-D/6-31G(d) (bottom)).

due to the poor resolution of the X-ray crystal structure (2.7 Å) of the reactivation complex of MetH-bound Co^{2+}Cbx that is the most reasonable crystal structure available for this complex and was used as a reference point in the present work. The closer analysis of MetH-bound Co^{2+}Cbx revealed that the axial H_2O ligand was engaged in a tightly coupled H-bonding network (Y1139--H_2O--E1097--R1094) with the local enzyme scaffold. Noteworthy were the direct H-bonding interactions between the axial H_2O ligand and the local Y1139 and E1097 residues where the axial ligand constructed a relatively stronger interaction with the E1097 residue (H_{H2O}--$^-OOC_{E1097}$ ~ 1.69 Å; O_{H2O}--HO_{Y1139} ~ 1.95 Å). This suggested that the E1097 residue might be exerting a pull effect on the axial ligand in order to disrupt its interaction with the

dx.doi.org/10.1021/ic201970k | Inorg. Chem. 2012, 51, 5533–5538

cofactor, which in turn would be facilitated by the proximal R1094 residue owing to its strong salt-bridge interaction with the E1097 residue (N_{R1094}-H--$^{-}OOC_{E1097}$ = 1.78 Å). This was consistent with the prior studies[13,15] suggesting that the local enzyme scaffold, especially the Y1139 and E1097 residues, promote the generation of a weakly coordinated square pyramidal MetH-bound Co^{2+}Cbx−OH_2 to combat the thermodynamic demand of the reduction process. It is important to mention that the axial H_2O ligand would be detached from Co^{2+}Cbx inside the enzyme environment only if the active site of MetH-bound Co^{2+}Cbx would be hydrophobic in nature. But since the tyrosine (Y1139), glutamate (E1097), and arginine (R1094) residues are present in the binding pocket of MetH-bound Co^{2+}Cbx, the active site would be strongly hydrophilic. As a result, the axial H_2O ligand would be retained in the active site.

DFT and QM/MM Analysis of Co^{+}Cbx Models. The axial H_2O ligand in the case of isolated Co^{+}Cbl structural models (Co^{+}Cbl--H_2O--H_2O and Co^{+}Cbl--H_2O--HOPh; Figure 4, Tables S3 and S4) was found to be H-bonded with the Co^{+} ion of the cofactor documenting the unusual H-bond forming feature of the d^8 Co^{+} ion. The binding Co^{+}--H-O motif in the optimized Co^{+}Cbl--H_2O--H_2O ($\angle Co^{+}$--H--O ∼ 157.9°) and Co^{+}Cbl--H_2O--HOPh ($\angle Co^{+}$−H--O ∼ 172.3°) complexes was found to be aligned in a strictly linear fashion, which is typical structural signature of H-bond forming systems. The axial H_2O ligand in the Co^{+}Cbl--H_2O--HOPh complex remained coordinated to the Co^{+} ion in contrast to the analogous Co^{2+}Cbl complex, where it was displaced by the tyrosine mimic (i.e., by PhOH). Notably the Co^{+}--O bond distance in the optimized H-bonded complexes (∼3.13−3.29 Å) was appreciably lengthened in comparison to the analogous Co^{2+}Cbl complexes, implying that the weakening of the Co^{2+}−O linkage was mandated to induce a conformational change at the axial ligand for forming a Co^{+}--H interaction and should not be misintrepreted as a mechanistic prerequisite for generating square planar Co^{+}Cbx. The optimized Co^{+}−H linkage in the Co^{+}Cbl--H_2O--HOPh complex (∼2.12−2.25 Å) was stronger than in the Co^{+}Cbl--H_2O--H_2O complex (∼2.18−2.37 Å) because the PhOH moiety, being a better H-donor, formed a stronger H-bonding contact with the axial H_2O ligand (PhOH--H_2O ∼1.72−1.79 Å) and exerted a noticeable push to strengthen the communication between the H_2O ligand and the Co^{+} ion.

The computed thermodynamic data for the isolated Co^{+}Cbl models further asserted the stable character of the Co^{+}--H interaction (Figure 5 and Tables S5−S8). The exothermicity affiliated with the H-bonded Co^{+}Cbl complexes was validated only upon treatement with the long-range- or the empirical dispersion-corrected functionals (Tables S5 and S7), which signified the presence of a sizable dispersion component in the Co^{+}--H interaction. The formation of a similar Co^{+}--H interaction has also been noted during a previous study,[14] but the thermodynamic feasibility of such a linkage could not be verified because the calculations were only performed using the conventional DFT functional (PBE/TZP). Upon solvation in chloroform (ε = 4.70), an appreciable degree of destabilization was caused to the Co^{+}--H linkage (Tables S6 and S8). As a result, the Co^{+}Cbl--H_2O--H_2O complex became endothermic at all levels of theory (Table S6), but the Co^{+}Cbl--H_2O--HOPh

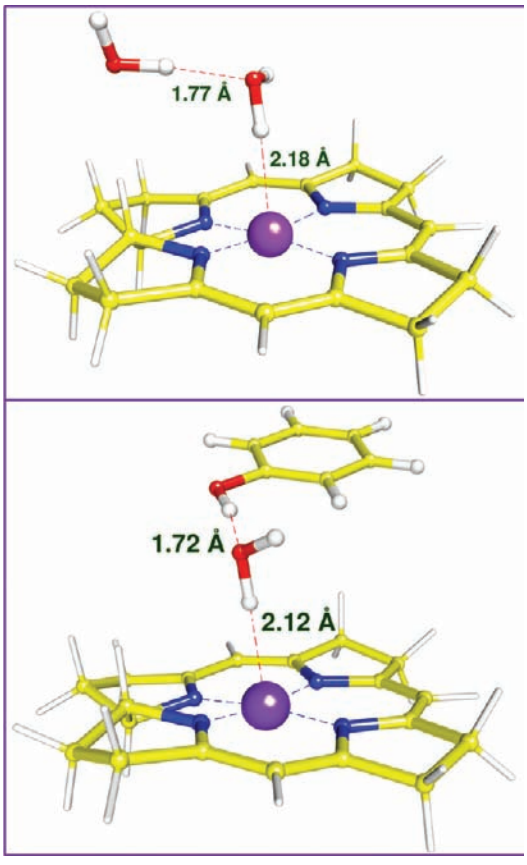

Figure 4. BP86-optimized Co^{+}Cbl--H_2O--H_2O (*upper*) and Co^{+}Cbl--H_2O--HOPh (*lower*).

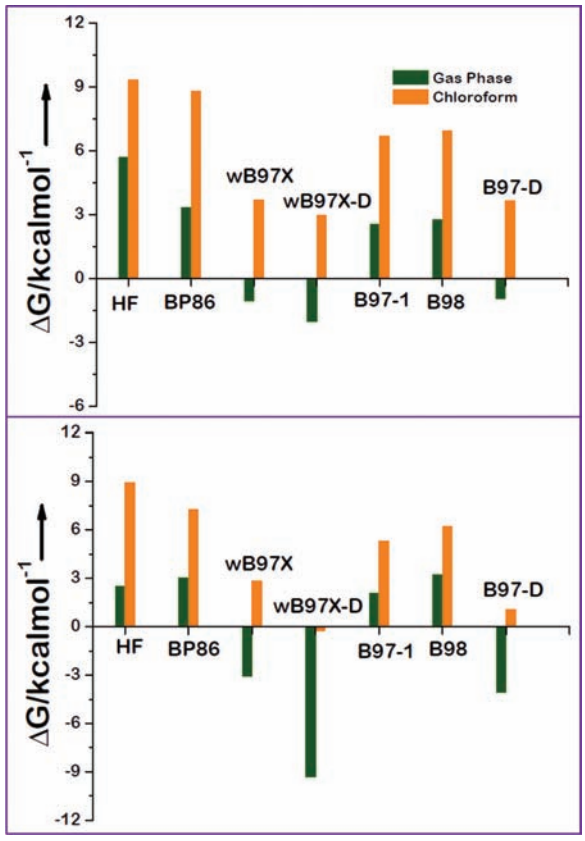

Figure 5. Computed Gibbs energy data for H-bonded Co^{+}Cbl--H_2O--H_2O (*upper*) and Co^{+}Cbl--H_2O--HOPh (*lower*).

dx.doi.org/10.1021/ic201970k | *Inorg. Chem.* 2012, 51, 5533−5538

complex, a realistic active site mimic of MetH-bound Co^{+}Cbx, remained a thermodynamically viable entity (Table S8), when analyzed with the dispersion-corrected functionals suggesting that the Co^{+}--H interaction could be engineered inside the enzyme scaffold of MetH. The AIM chemical tool could provide enriching quantitative insight into the precise nature of the Co^{+}--H interaction. Thus, as a next step, we performed an AIM analysis on the BP86 geometries of the Co^{+}Cbl--H_2O--H_2O and Co^{+}Cbl--H_2O--HOPh models. The electron density ($\rho_{Co^{+}\text{--}H}$) estimated at the bond critical point (BCP) of the Co^{+}--H interaction laid in the range of 0.02−0.03 e/au^3 (Table S9) that had usually been suggested for normal H-bonds.[39] This indicated that the Co^{+}--H interaction could be classified as a H-bond. The positive values of the Laplacian of electron density ($\nabla^2\rho_{Co^{+}\text{--}H}$) at the identified BCPs predicted the Co^{+}--H interaction to be a dominant electrostatic interaction. But it had been noted[40] that the total energy density (H) coupled with the Laplacian of the electron density ($\nabla^2\rho$) should be employed as a realistic descriptor of noncovalent interactions. The closer scrutiny of the AIM data instructed that the Co^{+}--H interaction was partially covalent rather than being purely electrostatic. But since the absolute $H_{Co^{+}\text{--}H}$ values were very small, the degree of partial covalence (electron sharing) should be treated as insignficant. It should be noted that the Co^{+}--H interaction could not be categorized as an agostic type because the transition metals that form such interactions are usually the early transition metals (e.g., Ti, Sc, Mo, etc.) in high oxidation states.[41] Apparently, the Co^{+} ion did not fall in this domain. On the other hand, the metal ion-induced H-bonds are formed by the late transition metals in low oxidation states such as Pt^{2+},[20,21] Ni^{2+},[42] Cu^{2+},[43] etc.[23] The Co^{+}--H interaction would clearly belong to this class.

Using the optimized structure of MetH-bound Co^{2+}Cbx as a starting point, a QM/MM analysis of MetH-bound Co^{+}Cbx was carried out to investigate whether the axial H_2O ligand would ligate to the Co^{+} ion via its O or H end. The computed QM/MM data clearly indicated the formation of a Co^{+}--H interaction in MetH-bound Co^{+}Cbx (Figure 6). The calculated Co^{+}--H bond distance (2.33−2.54 Å) was in the domain of d^8 metal ion-induced H-bonds.[20−23] Notably, the Co^{+}--H interaction was strengthened by ∼0.1−0.2 Å with the ωB97X and ωB97X-D functionals, which pointed out the presence of a noticeable dispersion component in the Co^{+}--H interaction.

The QM/MM estimated Co^{+}--H bond (∼2.33 Å−2.56 Å) was lengthened by ∼0.2−0.3 Å in comparison to that in the active site mimics (Co^{+}--H ∼ 2.18−2.37 Å (Co^{+}Cbl--H_2O--H_2O) and Co^{+}--H ∼ 2.12 − 2.39 Å (Co^{+}Cbl--H_2O−HOPh); Figure 4, Tables S3 and S4). The comparative analysis of the QM/MM optimized Co^{2+}Cbx and Co^{+}Cbx complexes suggested how the Co^{+}--H interaction could be formed inside the MetH enzyme. The free H end of the axial H_2O ligand in MetH-bound Co^{2+}Cbx might undergo a conformational change (i.e., rotatory motion toward the metal ion) leading to the formation of a H-bonded Co^{+}Cbx--H_2O complex. This conformational switch would be mainly driven by a change in the electronic configuration of the metal ion (i.e., Co^{2+} (d^7) → Co^{+} (d^8)), as no significant alteration was observed in the local environments of MetH-bound Co^{2+}Cbx and Co^{+}Cbx. As a result of the Co^{+}−H interaction, enzyme-bound Co^{+}Cbx might adapt to an alternative square pyramidal ligation geometry in addition to its commonly accepted square planar geometry.[13−16] Since the Co^{+}--H interaction-driven square pyramidal Co^{+}Cbx could tune the thermodynamics of the Co^{2+}/Co^{+} process,[22] the present QM/MM analysis might have

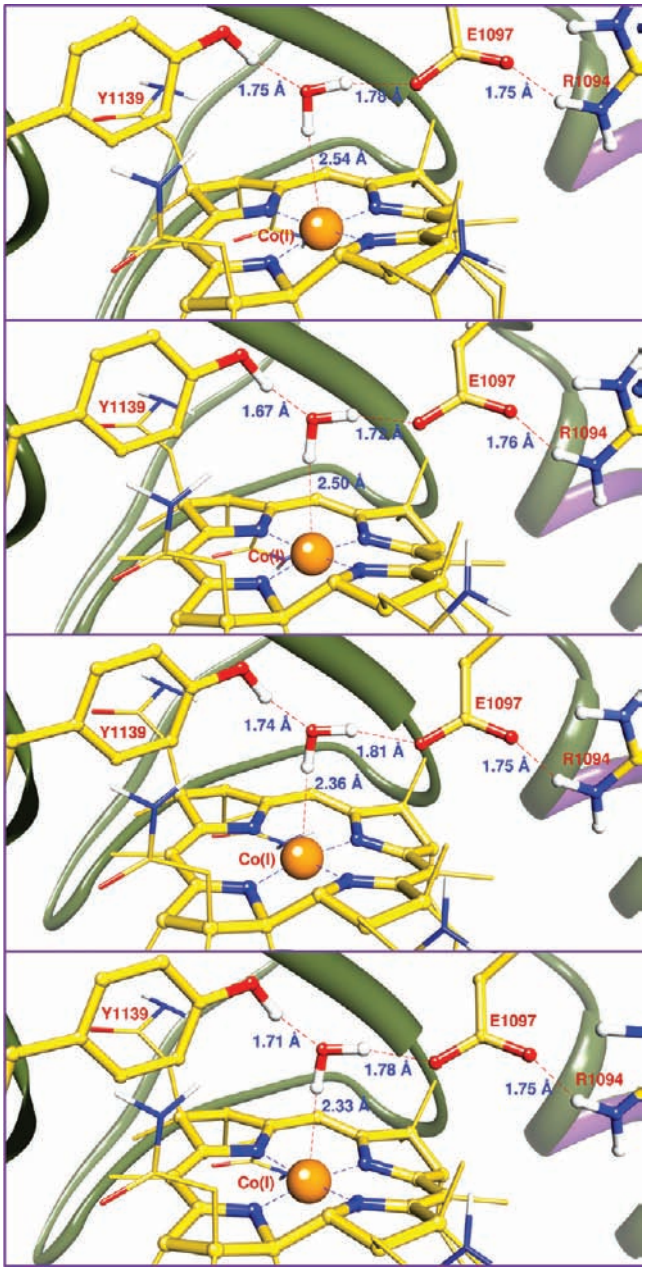

Figure 6. Active site view of the ONIOM (DFT:AMBER) optimized MetH-bound Co^{+}Cbx (DFT = B3LYP/6-31G(d) (top), BP86/6-31G(d) (middle 1), ωB97X/6-31G(d) (middle 2), and ωB97X-D/6-31G(d) (bottom)).

implications for the reactivation cycles of methyltransferases as well as for the adenosylation pathways of ACAs. It is worth mentioning that the X-ray crystallographic methods cannot elucidate the formation of a Co^{+}--H interaction because of their inability to resolve the electron density patterns associated with H-atoms. In order to experimentally validate the formation of a Co^{+}--H linkage, a neutron diffraction technique must be used, as has recently been demonstrated in the case of the *trans*-[$PtCl_2$-(NH_3)(N-glycine)]·H_2O complex. An early X-ray study[44] on this complex predicted that the axial H_2O ligand interacted with the Pt^{2+} center through its O end (Pt^{2+}−O = 3.52 Å), but a recent low temperature (20 K) neutron diffraction study[21] led to the precise description of hydrogens and illustrated that the axial H_2O ligand was rather H-bonded with the Pt^{2+} ion (Pt^{2+}--H = 2.89 Å).

dx.doi.org/10.1021/ic201970k | *Inorg. Chem.* 2012, 51, 5533−5538

We hope that our computational attempt would inspire an analogous neutron diffraction analysis of MetH-bound Co^{2+}Cbx and Co^{+}Cbx that would experimentally confirm the existence of a Co^{+}--H interaction.

CONCLUSION

In summary, the presented computational analysis suggested that a novel Co^{+}--H interaction might be operative during the reactivation cycle of the MetH enzyme. Benefitting from this associative interaction, MetH-bound Co^{+}Cbx would judiciously adapt to the square pyramidal coordination environment, which in turn might drive the otherwise inaccessible thermodynamically uphill Co^{2+}/Co^{+} reduction, a common chemical event in a variety of methyltransferases and ACAs.

ASSOCIATED CONTENT

Supporting Information

Active site close-up of the MetH-bound Co^{2+}Cbx complex, key structural features, computed thermodynamic data, and BCP properties of Co^{+}--H interaction. This material is available free of charge via the Internet at http://pubs.acs.org.

AUTHOR INFORMATION

Corresponding Author

*E-mail: pawel@louisville.edu.

Notes

The authors declare no competing financial interest.

ACKNOWLEDGMENTS

Acknowledgement is due to the Cardinal Research Cluster at University of Louisville for ensuring exceptional computational resources. H.H. thanks the Nanyang Assistant Professorship for financial support and the High Performance Computing Centre (HPCC) at Nanyang Technological University for computer resources.

REFERENCES

(1) Golding, C. W.; Postigo, D.; Matthews, R. G. *Biochemistry* **1997**, *36*, 8082−8091.
(2) Hagemeier, C. H.; Kruer, M.; Thauer, R. K.; Warkentin, E.; Ermler, U. *Proc. Natl. Acad. Sci. U.S.A.* **2006**, *103*, 18917−18922.
(3) Ragsdale, S. W.; Wood, H. G. *J. Biol. Chem.* **1985**, *260*, 3970−3977.
(4) Matthews, R. G.; Koutmos, M.; Datta, S. *Curr. Opin. Struct. Biol.* **2008**, *18*, 658−666.
(5) Escalante-Semerena, J. C.; Suh, S.-J.; Roth, J. R. *J. Bactriol.* **1990**, *172*, 273−280.
(6) Stich, T. A.; Buan, N. R.; Escalante-Semerena, J. C.; Brunold, T. C. *J. Am. Chem. Soc.* **2005**, *127*, 8710−8719.
(7) Maurice, M. St.; Mera, P. E.; Taranto, M. P.; Sesma, F.; Escalante-Semerena, J. C.; Rayment, I. *J. Biol. Chem.* **2007**, *282*, 2596−2605.
(8) Buan, N. R.; Suh, S-. J.; Escalante-Semerena, J. C. *J. Bactriol.* **2004**, *186*, 5708−5716.
(9) Herein, Co^{2+}Cbx and Co^{+}Cbx have been used as abbreviations for the full cob(II)alamin and cob(I)alamin, while Co^{2+}Cbl and Co^{+}Cbl represent their simplified versions.
(10) Lexa, D.; Savéant, J. M. *Acc. Chem. Res.* **1983**, *16*, 235−243.
(11) Vetter, H., Jr.; Knappe, J. *Z. Physiol. Chem.* **1971**, *352*, 433−446.
(12) Wolthers, K. R.; Scrutton, N. S. *J. FEBS* **2009**, *276*, 1942−1951.
(13) Koutmos, M.; Datta, S.; Pattridge, K. A.; Smith, J. L.; Matthews, R. G. *Proc. Natl. Acad. Sci. U.S.A.* **2009**, *106*, 18527−18532.
(14) Liptak, M. D.; Brunold, T. C. *J. Am. Chem. Soc.* **2006**, *128*, 9144−9156.
(15) Liptak, M. D.; Datta, S.; Matthews, R. G.; Brunold, T. C. *J. Am. Chem. Soc.* **2008**, *130*, 16374−16381.
(16) Stich, T. A.; Seravalli, J.; Venkateshrao, S.; Spiro, T. G.; Ragsdale, S. W.; Brunold, T. C. *J. Am. Chem. Soc.* **2006**, *128*, 5010−5020.
(17) Shi, S.; Daniels, L. M.; Espenson, J. H. *Inorg. Chem.* **1991**, *30*, 3407−3410.
(18) Hu, X. L.; Brunschwig, B. S.; Peters, J. C. *J. Am. Chem. Soc.* **2007**, *129*, 8988−8998.
(19) Voloshin, Y. Z.; Varzatskii, O. A.; Vorontsov, I. I.; Antipin, M. Y. *Angew. Chem., Int. Ed.* **2005**, *44*, 3400−3402.
(20) Kozelka, J.; Bergès, J.; Attias, R.; Fraitag, J. *Angew. Chem., Int. Ed.* **2000**, *39*, 198−201.
(21) Rizzato, S.; Bergès, J.; Mason, S. A.; Albinati, A.; Kozelka, J. *Angew. Chem., Int. Ed.* **2010**, *49*, 7440−7443.
(22) Kumar, M.; Kozlowski, P. M. *Angew. Chem., Int. Ed.* **2011**, *50*, 8705−8707.
(23) Braga, D.; Grepioni, F.; Tedesco, E.; Biradha, K.; Desiraju, G. R. *Organometallics* **1997**, *16*, 1846−1845.
(24) Jensen, K. P. *J. Phys. Chem. B* **2005**, *109*, 10505−10512.
(25) Kumar, N.; Prieto, M. A.; Rovira, C.; Lodowski, P.; Jaworska, M.; Kozlowski, P. M. *J. Chem. Theory Comput.* **2011**, *7*, 1541−1551.
(26) (a) Becke, A. D. *J. Chem. Phys.* **1986**, *84*, 4524−4529. (b) Perdew, J. P. *Phys. Rev. B* **1986**, *33*, 8822−8824.
(27) (a) Becke, A. D. *J. Chem. Phys.* **1997**, *107*, 8554−8560. (b) Hamprecht, F. A.; Cohen, A. J.; Tozer, D. J.; Handy, N. C. *J. Chem. Phys.* **1998**, *109*, 6264−6271.
(28) Schmider, H. L.; Becke, A. D. *J. Chem. Phys.* **1998**, *108*, 9624−9631.
(29) Grimme, S. J. *J. Comput. Chem.* **2006**, *27*, 1787−1799.
(30) Chai, J. -D.; Head-Gordon, M. *J. Chem. Phys.* **2008**, *128*, 084106.
(31) Chai, J. -D.; Head-Gordon, M. *Phys. Chem. Chem. Phys.* **2008**, *10*, 6615−6622.
(32) Frisch, M. J.; et al. *Gaussian 09*, revision C.02; Gaussian, Inc.: Wallingford, CT, 2009.
(33) Bader, R. F. W. *Atoms in Molecules: A Quantum Theory*; Oxford University Press: New York, 1990.
(34) Kristyan, S.; Pulay, P. *Chem. Phys. Lett.* **1994**, *229*, 175−180.
(35) Kräutler, B.; Keller, W.; Kratky, C. *J. Am. Chem. Soc.* **1989**, *111*, 8938−8940.
(36) (a) Li, H.; Robertson, A. D.; Jensen, J. H. *Proteins* **2005**, *61*, 704−721. (b) Bas, D. C.; Rogers, D. M.; Jensen, J. H. *Proteins* **2008**, *73*, 765−783.
(37) Besler, B. H.; Merz, K. M.; Kollman, P. A. *J. Comput. Chem.* **1990**, *11*, 431−439.
(38) The reported value of the Co^{2+}−O bond distance (3.60 Å) in ref 13 is different from its actual value (3.94 Å) in the PDB file (3IVA@2.7Å). Taking this into account, we have used 3.94 Å as the Co^{2+}−O bond distance.
(39) Popelier, P. *Atoms in Molecules: An Introduction*; Pearson Education: Harlow, England, 2000.
(40) Rozas, I.; Alkorta, I.; Elguero, J. *J. Am. Chem. Soc.* **2000**, *122*, 11154−11161.
(41) Brookharta, M.; Green, M. L. H.; Parkin, G. *Proc. Natl. Acad. Sci. U.S.A.* **2007**, *104*, 6908−6914.
(42) Keum, C.; Kim, C.; Kim, C.; Kwak, H.; Moonhee Kwon, M.; Namgung, H. *Bull. Korean Chem. Soc.* **1992**, *13*, 695−699.
(43) Thakur, T. S.; Desiraju, G. R. *Chem. Commun.* **2006**, 553−554.
(44) Baidina, I. A.; Podberezskaya, N. V.; Krylova, L. F.; Borisov, S. V. *J. Struct. Chem.* **1981**, *22*, 463−465.